

Improved fuzzy clustering algorithm with non-local information for image segmentation

Xiaofeng Zhang^{1,3} · Yujuan Sun¹ · Gang Wang¹ ·
Qiang Guo^{2,3} · Caiming Zhang^{2,3} · Beijing Chen⁴

Received: 25 September 2015 / Revised: 10 February 2016 / Accepted: 23 February 2016 /
Published online: 17 March 2016
© Springer Science+Business Media New York 2016

Abstract Fuzzy C-means(FCM) has been adopted to perform image segmentation due to its simplicity and efficiency. Nevertheless it is sensitive to noise and other image artifacts because of not considering spatial information. Up to now, a series of improved FCM algorithms have been proposed, including fuzzy local information C-means clustering algorithm(FLICM). In FLICM, one fuzzy factor is introduced as a fuzzy local similarity measure, which can control the trade-off between noise and details. However, the fuzzy factor in FLICM cannot estimate the damping extent of neighboring pixels accurately, which will result in poor performance in images of high-level noise. Aiming at solving

✉ Xiaofeng Zhang
iamzxf@126.com

Yujuan Sun
syj_anne@163.com

Gang Wang
happy_wg@163.com

Qiang Guo
guoqiang@sdufe.edu.cn

Caiming Zhang
czhang@sdu.edu.cn

Beijing Chen
48008543@qq.com

¹ School of Information and Electrical Engineering, Ludong University, Yantai, 264025, China

² School of Computer Science and Technology, Shandong University of Finance and Economics, Jinan, 250014, China

³ Shandong Provincial Key Laboratory of Digital Media Technology, Jinan, 250014, China

⁴ School of Computer & Software, Nanjing University of Information Science & Technology, Nanjing, 210044, China

this problem, this paper proposes an improved fuzzy clustering algorithm, which introduces pixel relevance into the fuzzy factor and could estimate the damping extent accurately. As a result, non-local context information can be utilized in the improved algorithm, which can improve the performance in restraining image artifacts. Experimental results on synthetic, medical and natural images show that the proposed algorithm performs better than current improved algorithms.

Keywords Fuzzy clustering · Image segmentation · FLICM · Pixel relevance · Non-local information

1 Introduction

Image segmentation is one of the most important techniques in image understanding and computer vision, and has been applied in many fields like object detection, video surveillance, medical imaging, etc [5, 7, 16, 18, 24, 26, 27, 30]. In essence, image segmentation is to partition one given image into homogeneous, non-overlapping regions with respect to some characteristics, such as gray value, texture and shape. Till now, image segmentation is still one bottleneck in digital image segmentation due to the complexity of images. For example, medical images suffer from partial volume effect(PVE), intensity inhomogeneity(IIH) [14, 15], and natural images suffer from image artifacts, which make the value of one pixel be affected by different objects in the image. Therefore, it is difficult to assign one single class to the affected pixels. For this reason, conventional “hard” segmentation methods are not suitable to segment these complex images, because they restrict each pixel exclusively to one class. As a result, fuzzy clustering has been extensively applied, for it admits one pixel belonging to several classes concurrently and can retain information as much as possible.

Of fuzzy clustering algorithms, FCM is a typical one, and has been widely applied in image segmentation for its simplicity and efficiency. FCM was first proposed by Dunn [11] and later extended by Bezdek [6]. As is well known, FCM performs well in noise-free images, while poor when noise, outliers or other image artifacts exist. This is because spatial information is not considered in the objective function [20–23]. To improve segmentation results in noisy images, various improved algorithms have been proposed. For example, bias-corrected version of FCM(BCFCM) was proposed by Ahmed [1], in which spatial information was incorporated into the objective function of FCM. In BCFCM, the impact of spatial information is weighted by one constant parameter α , the selection of which will affect the segmentation result greatly. To overcome this problem, Stelios and Chatzis proposed one parameter-free algorithm—FLICM [17], in which one fuzzy factor was defined to replace the parameter α in BCFCM. With the help of the fuzzy factor, the membership of neighbor pixels in one local window will converge to one similar value, whether the central pixel is contaminated or not.

In FLICM, the damping extent of neighbor pixels on the central one is based on the Euclidean distance between pixels, which makes FLICM perform poor in complex images. To improve the performance, FLICM was improved by introducing a trade-off weighted fuzzy factor and kernel method [12], termed as KWFLICM. However, only local information is utilized in FLICM and KWFLICM, and when the noise degree is high, both algorithms perform poor. To get satisfying segmentation results, one improved fuzzy clustering algorithm is proposed in this paper, in which pixel relevance will be utilized into the fuzzy factor to define the damping extent. Based on the novel fuzzy factor, non-local

information can be considered in the procedure of segmentation, which can well enhance the robustness while preserving image details, better than FLICM and KWFLICM.

The rest of this paper is organized as follows. In the next section, conventional FCM and typical improved algorithms are introduced. Section III introduces the proposed algorithm in detail, and then experimental results on various images are presented. Finally, a short but brief conclusion is drawn.

2 Related work

2.1 Conventional FCM

As is well known, FCM is one typical clustering algorithm in pattern recognition and machine learning. The target of FCM is to minimize the weighted distance between pixels and cluster centers. Formally,

$$F = \sum_{i=1}^C \sum_{j=1}^n u_{ij}^m d_{ij}^2 \quad (1)$$

where C is the predefined number of clusters, n is the number of pixels in the given image, u_{ij} is the membership of the j -th pixel belonging to the i -th cluster, and the constraint $\sum_{i=1}^C u_{ij} = 1$ is satisfied. $m \geq 1$ is the parameter to control the fuzziness of the clustering results, and $d_{ij} = \|x_j - v_i\|$ is one norm metric, denoting the Euclidean distance between the j -th pixel and the i -th cluster center. The membership and cluster centers are updated iteratively, and this process will stop when $\max |u_{ij}^{p+1} - u_{ij}^p| < \varepsilon$ or the predefined number of iterations is satisfied.

As is shown in (1), spatial information is not considered in FCM, which will make FCM sensitive to noise and other image artifacts. To solve this problem, many algorithms were proposed to improve the robustness to noise.

2.2 BCFCM and its variants

Bias-corrected version of FCM(BCFCM) was proposed by Ahmed [1], which improved FCM by adding one spatial term, and the label of one pixel was affected by those of neighbor pixels. Formally,

$$F = \sum_{i=1}^C \sum_{j=1}^n u_{ij}^m d_{ij}^2 + \frac{\alpha}{N_R} \sum_{i=1}^C \sum_{j=1}^n \sum_{r \in N_j} u_{ij}^m d_{ir}^2 \quad (2)$$

in which N_j is the neighbor window centering around pixel j , and N_R is its cardinality. The parameter α controls the effect of the neighbor term, which is usually determined by trial-and-error experiments.

In BCFCM, the neighbor information has to be computed in each iteration. Therefore, BCFCM is of low efficiency. To reduce the time complexity, Chen and Zhang proposed two variants of BCFCM, named FCMS1 and FCMS2 [9], in which the neighbor information was replaced with the information in the median-filtered image or mean-filtered image. Formally,

$$F = \sum_{i=1}^C \sum_{j=1}^n u_{ij}^m \|x_j - v_i\|^2 + \alpha \sum_{i=1}^C \sum_{j=1}^n u_{ij}^m \|\bar{x}_j - v_i\|^2 \quad (3)$$

where \bar{x}_j is intensity of the j -th pixel in the mean-filtered image or the median-filtered image, corresponding to FCMS1 or FCMS2, respectively.

As is well known, the mean-filtered image and the median-filtered image can be computed in advance, making FCMS1 and FCMS2 have low time complexity in comparison with BCFCM. Moreover, since the mean filter and median filter are robust to Gaussian noise or Salt & Pepper noise, so are FCMS1 and FCMS2.

2.3 EnFCM

To speed up the process of image segmentation, Szilagyi et al. proposed an enhanced FCM (EnFCM)[25]. Before segmentation, one linearly-weighted sum image ξ between the original image and its mean-filtered image is firstly calculated by

$$\xi_i = \frac{1}{1 + \alpha} \left(x_i + \frac{\alpha}{N_R} \sum_{j \in N_i} x_j \right) \tag{4}$$

where α has the same role as that in BCFCM. Based on the histogram of ξ , the objective function of EnFCM can be defined as

$$F = \sum_{i=1}^C \sum_{j=1}^L \gamma_j u_{ij}^m (\xi_j - v_i)^2 \tag{5}$$

where L is the number of gray levels of the image ξ , γ_j is the number of pixels with intensity value j . Usually, the number of gray levels is much smaller than that of pixels. As a result, the efficiency of EnFCM is much higher than that of other algorithms.

2.4 Fast generalized fuzzy C-means clustering(FGFCM)

Due to the difficulty of selecting the parameter α in (4), EnFCM cannot retrieve better results in most medical and natural images. To overcome this, Cai et al. proposed FGFCM [8], which was motivated by the idea of EnFCM. Similarly, FGFCM performs segmentation with the help of the histogram of the sum image. Different from EnFCM which is based on the linearly weighted sum image, FGFCM is based on the non-linearly weighted sum image. In FGFCM, one local pixel similarity measure S_{ij} is defined, which incorporates both the local gray information and local spatial information. Formally,

$$\xi_j = \frac{\sum_{r \in N_j} S_{jr} x_r}{\sum_{r \in N_j} S_{jr}} \tag{6}$$

In FGFCM, the similarity between the center pixel j and neighbor pixel r is defined as

$$S_{jr} = S_{jr}^S \times S_{jr}^G \tag{7}$$

where S_{jr}^S and S_{jr}^G are spatial similarity and gray similarity, respectively. In FGFCM, S_{jr}^S and S_{jr}^G are defined as

$$S_{jr}^S = \exp\{-\max(|p_j - p_r|, |q_j - q_r|)/\lambda_S\} \tag{8}$$

$$S_{jr}^G = \exp\left\{-\frac{(x_j - x_r)^2}{\lambda_G \sigma_j^2}\right\} \tag{9}$$

where (p_j, q_j) is the spatial coordinate of pixel j , λ_S and λ_G are scale parameters of gray and spatial information, and σ_j is the variance of those pixels centering around the j -th

pixel. FGFCM provides good segmentation results in images of low-level noise, but the selection of parameters is one difficult task, just as that in BCFCM and EnFCM.

2.5 Fuzzy local information C-means algorithm (FLICM)

In image segmentation, it is very difficult to balance between noise insensitiveness and image details. In the improved algorithms mentioned above, this task is accomplished by adjusting corresponding parameters, which is very difficult for complex images. Aiming at this problem, Krinidis and Chatzis proposed one parameter-free algorithm—FLICM [17]. In FLICM, one fuzzy factor G_{ki} was introduced, which played the role of α in the improved algorithms mentioned above and could well control the tradeoff between noise insensitiveness and image detail preservation. Moreover, different from the other improved algorithms, FLICM is free of parameters. In FLICM, the fuzzy factor is defined as

$$G_{ij} = \sum_{r \in N_j} \frac{1}{d_{jr} + 1} (1 - u_{ir})^m \|x_r - v_i\|^2 \quad (10)$$

in which d_{jr} is the Euclidean distance between pixel j and pixel r . With the application of fuzzy factor G_{ij} , the corresponding membership values of the non-noisy pixels, as well as the noisy pixels that falling into the local window will converge to a similar value, and thereby balance the membership values of the pixels that located in the window [12]. In FLICM, the objective function is defined as

$$F = \sum_{i=1}^C \sum_{j=1}^n [u_{ij}^m (x_j - v_i)^2 + G_{ij}] \quad (11)$$

The membership and cluster centers can be updated iteratively by minimizing the objective function in (11), formalized as

$$u_{ij} = \frac{1}{\sum_{k=1}^C \left(\frac{\|x_j - v_i\|^2 + G_{ij}}{\|x_j - v_k\|^2 + G_{kj}} \right)^{1/(m-1)}} \quad (12)$$

$$v_i = \frac{\sum_{j=1}^n u_{ij}^m x_j}{\sum_{j=1}^n u_{ij}^m} \quad (13)$$

3 Proposed Method

As is mentioned before, one fuzzy factor is introduced into FLICM to replace α in BCFCM, making FLICM free of parameters. In the fuzzy factor, the influence of neighbor pixels on the central one, also called the damping extent, is exerted flexibly by using their Euclidean distance from the central one [13]. If the distance is small, the damping extent on the central pixel is big, otherwise it is small. In the procedure of image segmentation, the membership of pixels having big damping extent on the central one, together with that of the central pixel, will converge to similar values. But when the central pixel is noisy, it fails to analyze the impact of neighbor pixels, for it is not conformity with the discrepancy between neighbor pixels. To overcome this, KWFLICM was proposed by using local coefficient of variation and kernel function. However, in complex images, especially those of high-level

noise, FLICM and KWFLICM perform poor. This paper holds the idea that the reason is that only local information is utilized in the two algorithms.

As is well known, there is much information that can be utilized in the segmentation, not limited to local ones. For example, there are many pixels with similar neighborhood configuration to one given pixel, and these pixels should be utilized to enhance the robustness of FLICM. However, these pixels don't exist in the neighbor window and cannot be considered in FLICM and KWFLICM. To overcome this, one improved algorithm will be presented in this section, in which pixel relevance will be adopted to measure the damping extent. With the help of pixel relevance, non-local information in the whole image can be considered, which can improve the robustness to image artifacts.

3.1 Pixel relevance

Compared with those algorithms using local information, the algorithm utilizing the pixels with similar configurations to guide the segmentation is preferable. As is well known, considering more information means low efficiency. To balance the segmentation quality and efficiency, one search window centering around the given pixel will be defined, and only the pixels in the window with similar configuration will play a positive role in guiding the procedure of image segmentation. As is analyzed above, measuring the similarity between pixels accurately is very important, which will be termed as pixel relevance in the proposed algorithm. The phrase “non-local” means that the number of pixels considered in this paper is bigger than that in other improved local algorithms, since the radius of the search window can be big enough to cover all pixels in this image.

Formally, the search window around the i -th pixel is represented as W_i^r , and the height and width of W_i^r is $(2r + 1)$. In the proposed algorithm, all information provided by pixels in W_i^r will be considered. In this paper, pixel relevance between the two pixels i and $j \in W_i^r$ is denoted as $S(i, j)$, and is defined as

$$S(i, j) = \frac{1}{Z_i} \exp\left(-\frac{\|X_{N_i} - X_{N_j}\|^2}{h^2}\right) \quad (14)$$

in which N_i and N_j are two image patches centering around the i -th and j -th pixel (the size of image patch is assigned 3×3 in this paper), h is the filtering degree parameter, controlling the decay of $S(i, j)$. Z_i is the normalizing factor, defined as

$$Z_i = \sum_{j \in W_i^r} \exp\left(-\frac{\|X_{N_i} - X_{N_j}\|^2}{h^2}\right) \quad (15)$$

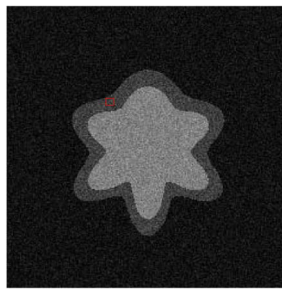
As is analyzed in [29], h is very crucial to the segmentation results and the selection of this parameter is often done manually. To overcome this problem, h is determined adaptively instead of using a single value for all the pixels. Concretely, h is calculated based on the statistical characteristics in its search window, which is called self-tuning [28].

$$h = \sqrt{\left(\sum_{r \in N_i} (x_r - x_i)^2\right) / N_R} \quad (16)$$

where N_i is the set of pixels in W_i^r , and N_R is its cardinality. In addition, the patches are often with different geometrical structures due to the positions of pixels. To compute pixel relevance accurately, the geometrical structures of X_{N_i} and X_{N_j} in this paper are supposed to be the same, which can make the improved algorithm more robust to image artifacts.

According to the definition in (14) and (15), $0 \leq S(i, j) \leq 1$ and $\sum_{j \in N_i} S_{ij} = 1$ hold. If X_{N_i} and X_{N_j} are similar, the pixel relevance S_{ij} is close to 1, otherwise, S_{ij} is close to 0.

Let's take one example in Fig. 1a to illustrate the computation of pixel relevance. The intensities of pixels in the red box is tabulated in Fig. 1b, and corresponding pixel relevances between the central pixel(the central one with intensity value 66) and the pixels in the search window are presented in Fig. 1c. According to (14), the value of pixel relevance between the pixel in the search window and the central pixel depends on the similarity between corresponding patches. As is shown in Fig. 1c, pixel relevance between A and the central pixel is larger than that between B and the central pixel, even though the distance between A and the central pixel is larger than that between B and the central pixel. The same situation happens to C and D, as is shown in Fig. 1b and c.



(a)

	C	D					
82	80	64	58	68	93	58	
61	A	75	70	63	72	91	65
62	77	75	67	73	57	73	
63	B	63	61	66	77	45	62
89	76	76	90	98	59	55	
77	61	58	63	56	63	68	
69	49	43	67	111	113	137	

(b)

0.0013	7.9850e-004	2.5602e-004	0.0011	0.0198	8.9780e-004	2.0258e-007
0.0061	0.0203	0.0049	0.0127	2.4731e-004	5.1914e-005	6.8736e-006
0.0010	5.7235e-004	7.1208e-004	0.0127	1.3961e-005	9.2140e-006	4.9797e-006
0.0316	0.0169	0.1749		1.0267e-004	6.9104e-006	1.3585e-007
1.2538e-004	4.3313e-005	1.3763e-004	7.8529e-006	1.7311e-007	3.8457e-006	7.7079e-006
1.0233e-006	1.8307e-007	3.9496e-006	7.9929e-005	0.0011	7.1539e-006	3.0481e-008
0.0032	2.9750e-005	3.5246e-004	1.4059e-004	3.9324e-007	3.7442e-014	1.9006e-018

(c)

Fig. 1 Pixel relevance based on non local information(the radius of W'_i is 7). **a** image with noise; **b** intensities of pixels in the red box; **c** pixel relevance between the central pixel and those in the search window

3.2 Description of the proposed algorithm

In FLICM, the damping extent of neighbor pixels on the central one will make the membership of pixels in local window converge to similar values, making FLICM robust to image artifacts. However, there are two shortages of FLICM: (1) since the damping extent is measured by the Euclidean distance, the irrelevant pixels in local window should also have similar membership values, which is unreasonable; (2) only local information is considered in FLICM, resulting in poor performance. The first problem is solved by KWFLICM by introducing one trade-off weighted fuzzy factor and kernel function. However, information adopted in KWFLICM is also limited to local context, which will make KWFLICM perform poor in complex images. Aiming at this problem, FLICM will be improved by non-local information, which can enhance the robustness of the algorithm in complex images.

According to (10), neighbor pixels will have larger damping extent on the central pixel than faraway pixels, which will make neighbor pixels have similar membership with that of the central one. Based on this principle, FLICM can be improved to make the memberships of relevant pixels converge to similar values. Formally, if $S(i, j)$ between the i -th pixel and $j \in W_i^r$ is large, the damping extent of the j -th pixel on the i -th pixel should be big, and vice versa. Therefore, the membership of the two pixels will converge to similar values, and in turn enhance the robustness of the proposed algorithm. Based on the analysis, the fuzzy factor in the proposed algorithm can be defined as follows.

$$G_{ij} = \sum_{k \in w_j^r} S(j, k)(1 - u_{ik})^m \|x_k - v_i\|^2 \quad (17)$$

Compared with FLICM, the proposed algorithm has several improvements, summarized as follows.

- (1) the Euclidean distance is removed from fuzzy factor, and faraway pixels with similar configurations can also play positive role on the central one;
- (2) pixel relevance is introduced into the fuzzy factor to measure the damping extent, which is defined as the patch similarity between corresponding pixels;
- (3) one search window W_j^r is defined to replace N_j , and non-local information can be considered.

In the proposed algorithm, pixel relevance is defined as the patch similarity between corresponding pixels, with the help of which non-local information can be considered into the fuzzy factor to measure the damping extent. Therefore, the proposed algorithm is denoted as NLFCM, and the framework is illustrated in Algorithm 1. Also, the updating equations of membership and cluster centers in the proposed algorithm are also the same as those in FLICM.

Algorithm 1 The framework of NLFCM.

- Step 1. Compute pixel relevance between pixel i and $j \in W_i^r$ by Eq.(14);
 - Step 2. Initialize the fuzzy partition matrix u^0 at random, satisfying $0 \leq u_{ij} \leq 1$ and $\sum_{i=1}^C u_{ij} = 1$;
 - Step 3. Set the iterator counter $it = 1$;
 - Step 4. Compute cluster centers by Eq.(13);
 - Step 5. Compute the fuzzy factor by Eq.(17);
 - Step 6. Update the fuzzy partition matrix u^{it} by Eq.(12);
 - Step 7. If $\max\{|u^{it} - u^{it-1}|\} < \varepsilon$ or $it = \maxIter$ holds, Algorithm ends, else $it = it + 1$, goto Step 4;
-

When the algorithm has converged, a defuzzification process takes place to convert the fuzzy image to the crisp segmented image. In a general way, the maximum membership procedure method is adopted. This procedure assign the j -th pixel to the k -th class with the highest membership. Formally,

$$k = \arg\{\max\{u_{kj}\}\} \quad (k = 1, 2, \dots, C) \quad (18)$$

4 Experimental Study

This section will present the experimental results on different images, including three synthetic images, three medical images and three natural images. To illustrate the robustness of the proposed algorithm, these images are contaminated with different types of noise. We will compare the proposed algorithm with several FCM-related ones: FCM, BCFCM, FCMS1, FCMS2, EnFCM, FGFCM, FLICM and KWFLICM. For all compared algorithms, we set $m = 2$, $\varepsilon = 10^{-5}$ and 3×3 neighborhood is adopted for local search. In BCFCM, FCMS1, FCMS2 and EnFCM, α is assigned 2. In FGFCM, λ_G and λ_S are assigned 2 and 3 respectively.

4.1 Results on synthetic images

The first experiment applies the algorithms on three synthetic test images, which could be obtained from [12]. The first image with 128×128 pixels includes two classes of two intensity values taken as 20 and 120, as shown in Fig. 2a. The other two images with $256 \times$

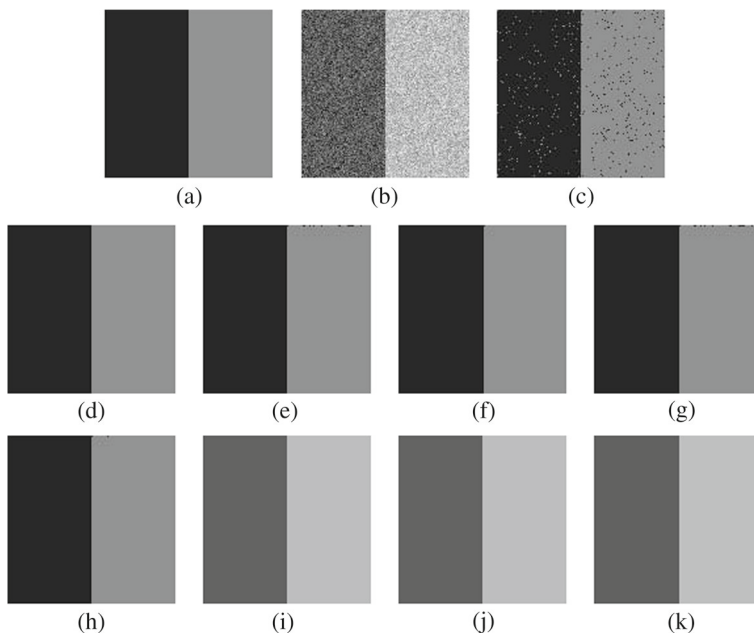


Fig. 2 Segmentation results of the first synthetic image. **a** Original image. **b** Noisy image corrupted by Gaussian noise of level 20%. **c** FCM result. **d** BCFCM result. **e** FCMS1 result. **f** FCMS2 result. **g** EnFCM result. **h** FGFCM result. **i** FLICM result. **j** KWFLICM result. **k** NLFCM result

256 pixels and 244×244 pixels, including four intensity values taken as 0, 85, 170 and 255, are presented in Figs. 3a and 4a, respectively. To assure the efficiency of the proposed algorithm, the size of the search window is assigned as 7×7 , and the selection of the radius will be discussed later.

Considering the existence of different types of noise in the synthetic image, segmentation accuracy (SA) is adopted to evaluate the effect of the algorithms, which is defined as the sum of the pixels correctly classified divided by the number of all pixels. Formally,

$$SA = \frac{\sum_{i=1}^C A_i \cap C_i}{\sum_{j=1}^C C_j} \quad (19)$$

where A_i is the set of pixels belonging to the i -th class found corresponding algorithm, C_i is the set of pixels belonging to the i -th class in the reference image.

To compare these algorithms furthermore, two cluster validity functions are selected to evaluate the algorithms, which are the partition coefficient V_{pc} [4] and the partition entropy V_{pe} [3]. Formally,

$$V_{pc} = \sum_{i=1}^C \sum_{j=1}^n u_{ij}^2 / n \quad (20)$$

$$V_{pe} = - \sum_{i=1}^C \sum_{j=1}^n (u_{ij} \log u_{ij}) / n \quad (21)$$

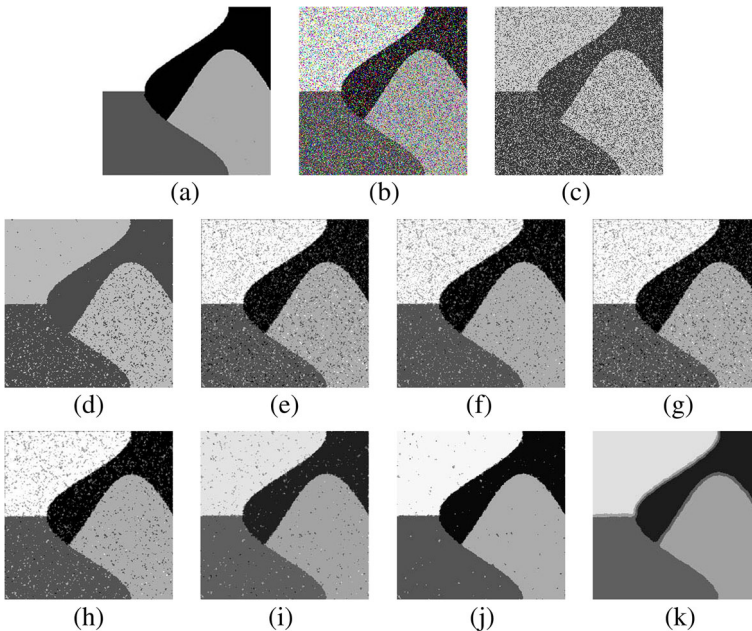


Fig. 3 Segmentation results of the second synthetic image. **a** Original image. **b** Noisy image corrupted by Salt & Pepper noise of level 30%. **c** FCM result. **d** BCFCM result. **e** FCMS1 result. **f** FCMS2 result. **g** EnFCM result. **h** FGFCM result. **i** FLICM result. **j** KWFLICM result. **k** NLFCM result

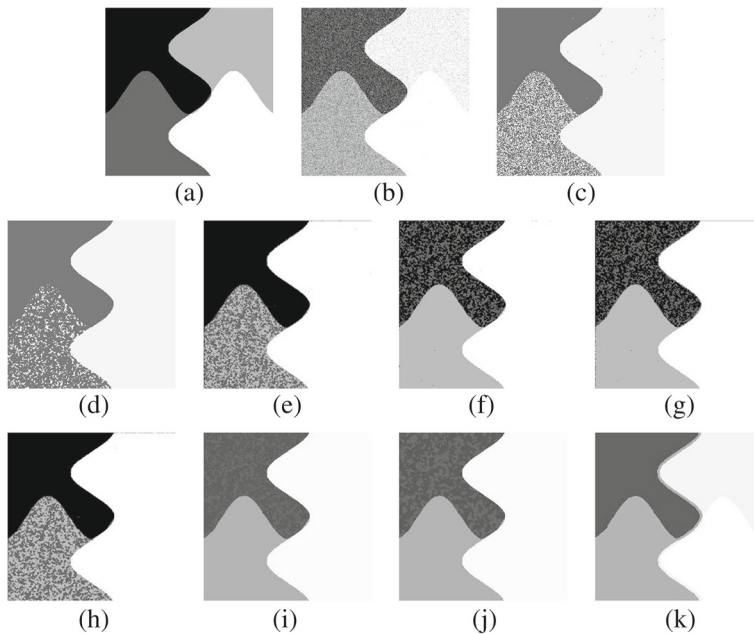


Fig. 4 Segmentation results of the third synthetic image. **a** Original image. **b** Noisy image corrupted by Gaussian noise of level 30%. **c** FCM result. **d** BCFCM result. **e** FCMS1 result. **f** FCMS2 result. **g** EnFCM result. **h** FGFCM result. **i** FLICM result. **j** KWFLICM result. **k** NLFCM result. It needs to be clear that there are 4 clusters in the result of NLFCM, of which the two in the right part need to be distinguished carefully

where n is the number of pixels in the given image. The final partition of the image with less fuzziness means better performance. Hence, the best clustering is achieved when V_{pc} is maximal and V_{pe} is minimal.

Fig. 2c–k presents the segmentation results of the nine algorithms for Fig. 2b, which is corrupted by Gaussian noise of level 20%. It needs to explain that the intensities of pixels in our experiments are assigned as the value of corresponding cluster center, and the segmentation results may have different color. Obviously, the ideal segmentation result is to be the same as Fig. 2a. However, noise still exists in the segmentation results of FCM, FCMS1, FCMS2, EnFCM and FGFCM, as is obviously shown in Fig. 2c–k. The results of the five algorithms without spatial information or with local spatial information are not satisfying. On the contrary, the results of BCFCM, FLICM, KWFLICM and NLFCM proposed in this paper are excellent, and almost all noise is removed in the process of segmentation.

Table 1 tabulates the comparison of the segmentation accuracy of these nine algorithms on noisy images corrupted by Gaussian noise and Salt & Pepper noise with varying degrees. It needs to be noted that the SA value is the average value of ten runs. In our experiments, the noise degrees are adopted 15%, 20% and 30%. It can be seen from Table 1 that the SAs of FLICM, KWFLICM and NLFCM are much better than those of the other algorithms. What's more, the SAs of these three algorithms are more stable.

The segmentation results on the other two synthetic images are presented in Figs. 3 and 4. There are 256×256 and 244×244 pixels in the two synthetic images, contaminated with Salt & Pepper noise(30%) and Gaussian noise(30%) respectively. As is shown in Fig. 3, there is still much noise in the results of FCM, BCFCM, FCMS1, FCMS2, EnFCM

Table 1 Segmentation accuracy(SA%) on the first synthetic image with different noise

Noise	FCM	BCFCM	FCMS1	FCMS2	EnFCM	FGFCM	FLJCM	KWFLJCM	NLFCM
Gaussian 15%	97.854	99.986	99.975	99.981	99.975	99.994	99.969	99.988	99.999
Gaussian 20%	97.571	99.986	99.913	99.994	99.913	99.988	99.945	99.982	99.998
Gaussian 30%	97.351	99.988	99.851	99.988	99.857	99.988	99.786	99.878	99.995
Salt & Pepper 15%	92.572	94.214	94.259	95.914	94.184	99.070	99.652	99.951	99.980
Salt & Pepper 20%	89.777	91.681	92.107	94.519	91.754	98.345	99.206	99.902	99.915
Salt & Pepper 30%	84.570	85.822	85.790	90.508	85.783	94.265	99.231	99.780	99.841

Table 2 Comparison of Partition coefficient V_{pc} on the synthetic images with different noise

Image	Noise	FCM	BCFCM	FCMSI	FCMS2	EnFCM	FGFCM	FLICM	KWFLICM	NLFCM
Fig. 2a	Gaussian 15%	0.8993	0.8902	0.9430	0.9468	0.9707	0.9770	0.9114	0.9490	0.9849
	Gaussian 20%	0.8970	0.8884	0.9413	0.9449	0.9692	0.9750	0.9102	0.9484	0.9849
	Gaussian 30%	0.8957	0.8855	0.9389	0.9434	0.9672	0.9737	0.9091	0.9475	0.9844
	Salt & Pepper 15%	0.9556	0.7572	0.8864	0.9463	0.9287	0.9782	0.9037	0.9615	0.9788
	Salt & Pepper 20%	0.9381	0.6934	0.8543	0.9260	0.9112	0.9658	0.8748	0.9486	0.9695
	Salt & Pepper 30%	0.8747	0.5835	0.7887	0.8827	0.8779	0.9365	0.804	0.9213	0.9653
Fig. 3a	Gaussian 15%	0.8833	0.8777	0.8090	0.8112	0.9584	0.8658	0.8493	0.9455	0.9641
	Gaussian 20%	0.8864	0.8792	0.9090	0.8029	0.9497	0.8585	0.7200	0.9410	0.9619
	Gaussian 30%	0.8872	0.8723	0.8720	0.8813	0.9256	0.9324	0.7599	0.9061	0.9537
	Salt & Pepper 15%	0.8658	0.7874	0.8122	0.8802	0.8875	0.9464	0.7261	0.8445	0.9466
	Salt & Pepper 20%	0.8645	0.7600	0.7594	0.8378	0.8591	0.9183	0.6478	0.7927	0.9191
	Salt & Pepper 30%	0.8628	0.6999	0.6551	0.7385	0.8104	0.8569	0.4863	0.6745	0.9058
Fig. 4a	Gaussian 15%	0.6999	0.8640	0.7665	0.7691	0.8414	0.9421	0.7980	0.9130	0.9496
	Gaussian 20%	0.8834	0.8632	0.8787	0.8806	0.9346	0.9421	0.6921	0.9040	0.9574
	Gaussian 30%	0.8911	0.8600	0.8252	0.8342	0.9046	0.9114	0.7353	0.8371	0.9423
	Salt & Pepper 15%	0.8853	0.7646	0.7995	0.9207	0.8779	0.9618	0.7375	0.8627	0.8942
	Salt & Pepper 20%	0.8901	0.7298	0.7406	0.8907	0.8456	0.9404	0.6565	0.8162	0.8759
	Salt & Pepper 30%	0.9010	0.6619	0.6431	0.8308	0.8044	0.8958	0.5097	0.7207	0.8452

Table 3 Comparison of Partition entropy V_{pe} on the synthetic images with different noise

Image	Noise	FCM	BCFCM	FCMS1	FCMS2	EnFCM	FGFCM	FLICM	KWFLICM	NLFCM
Fig. 2a	Gaussian 15%	0.2594	0.3110	0.1700	0.1652	0.0919	0.0778	0.2564	0.1558	0.0447
	Gaussian 20%	0.2641	0.3152	0.1742	0.1700	0.0956	0.0833	0.2591	0.1573	0.0449
	Gaussian 30%	0.2667	0.3215	0.1797	0.1731	0.1003	0.0859	0.2617	0.1594	0.0457
	Salt & Pepper 15%	0.1264	0.5390	0.2802	0.1155	0.1906	0.0569	0.2585	0.1022	0.0552
	Salt & Pepper 20%	0.1731	0.6677	0.3490	0.1589	0.2292	0.0876	0.3232	0.1352	0.0811
	Salt & Pepper 30%	0.3099	0.8684	0.4868	0.2545	0.3042	0.1621	0.4757	0.2035	0.0938
Fig. 3a	Gaussian 15%	0.3023	0.3301	0.5563	0.5474	0.1397	0.4120	0.4833	0.1877	0.1208
	Gaussian 20%	0.2885	0.3181	0.2812	0.5633	0.1601	0.4253	0.8026	0.1997	0.1161
	Gaussian 30%	0.2697	0.3083	0.3621	0.3363	0.2257	0.2041	0.6836	0.2810	0.1391
	Salt & Pepper 15%	0.3566	0.5178	0.5482	0.3375	0.3377	0.1690	0.8157	0.4864	0.2381
	Salt & Pepper 20%	0.3557	0.5683	0.6873	0.4569	0.4132	0.2502	1.01638	0.6326	0.2457
	Salt & Pepper 30%	0.3537	0.6768	0.9521	0.7278	0.5375	0.4181	1.4081	0.9482	0.3051
Fig. 4a	Gaussian 15%	0.6768	0.3486	0.6470	0.6401	0.4632	0.1864	0.6176	0.2893	0.1685
	Gaussian 20%	0.2873	0.3425	0.3686	0.3643	0.2071	0.1864	0.8772	0.3121	0.1340
	Gaussian 30%	0.2628	0.3298	0.4888	0.4524	0.2787	0.2617	0.7474	0.4553	0.1755
	Salt & Pepper 15%	0.3081	0.5556	0.5791	0.2103	0.3705	0.2134	0.7735	0.4253	0.2396
	Salt & Pepper 20%	0.2933	0.6192	0.7329	0.2907	0.4518	0.1760	0.9868	0.5594	0.2875
	Salt & Pepper 30%	0.2609	0.7392	0.9807	0.4521	0.5512	0.3022	1.3564	0.8206	0.2921

and FGFCM, while a small portion of noise in the results of FLICM and KWFLICM. Compared with the former eight algorithms, NLFCM can remove almost all the noise, and the segmented regions are also homogeneous, meaning that NLFCM is with higher SA and performs better than other algorithms.

The partition coefficient V_{pc} and the partition entropy V_{pe} on the three synthetic images contaminated by Gaussian noise or Salt & Pepper noise with varying degrees are compared in our experiments, presented in Tables 2 and 3. It needs to be noted that the values of V_{pc} and V_{pe} are the average values of ten runs.

As is shown in Tables 2 and 3, the V_{pc} and V_{pe} values of NLFCM are comparable to or even better than those of the other algorithms on the images corrupted by Gaussian noise. When the given image is contaminated by Salt & Pepper noise, the V_{pc} and V_{pe} values of NLFCM are not so well. However, when Salt & Pepper noise is added to the image, the results retrieved by the other algorithms cannot be accepted. Comparatively, the result of NLFCM is satisfying, and the segmented regions are more homogeneous, which can be seen from Figs. 3c–k and 4c–k.

4.2 Results on medical images

In this subsection, three magnetic resonance(MR) images are involved in our experiment to evaluate the nine algorithms. As is well known, MR images are usually contaminated

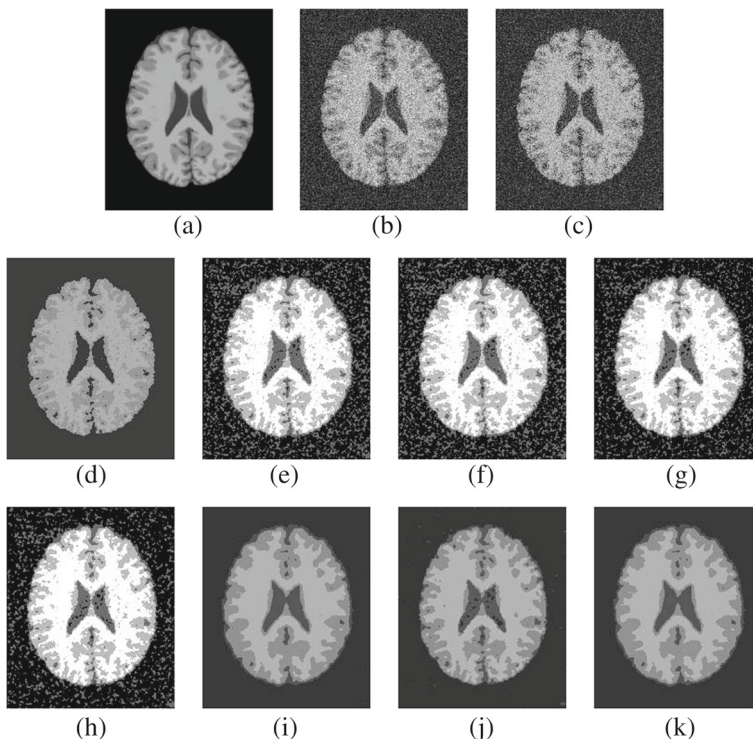


Fig. 5 Segmentation Results of one medical image corrupted by 10% Rician noise. **a** Original image. **b** Noisy image corrupted by Rician noise of level 30%. **c** FCM result. **d** BCFCM result. **e** FCMS1 result. **f** FCMS2 result. **g** EnFCM result. **h** FGFCM result. **i** FLICM result. **j** KWFLICM result. **k** NLFCM result

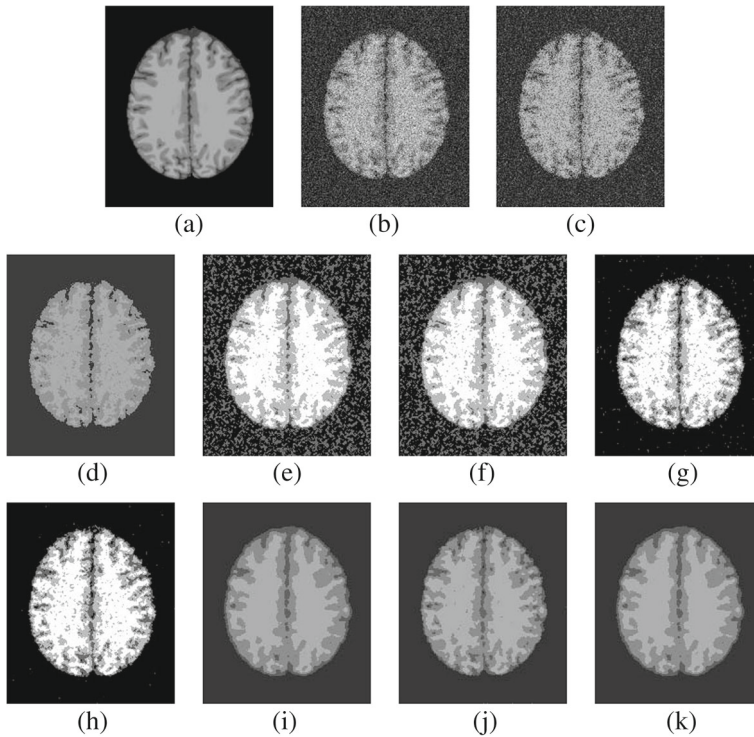


Fig. 6 Segmentation results of another medical image corrupted by 30% Rician noise. **a** Original image. **b** Noisy image corrupted by Rician noise of level 30%. **c** FCM result. **d** BCFCM result. **e** FCMS1 result. **f** FCMS2 result. **g** EnFCM result. **h** FGFCM result. **i** FLICM result. **j** KWFLICM result. **k** NLFCM result

by Rician noise [29], resulting in the existence of partial volume effect(PVE) and intensity inhomogeneity(IIH) [14, 15]. Of the three images, two are from BrainWeb images [10], and the other is from [17], illustrated in Figs. 5a, 6a and 7a. There are 181×217 pixels in Figs. 5a and 6a, while 256×255 pixels in Fig. 7a. In our experiments, Rician noise is generated by a code obtained from Ged Ridgway[19], and the first two images are corrupted by 30 % Rician noise($s = 30$), and the third image is corrupted by 10 % Rician noise($s = 10$), shown in Figs. 5b, 6b and 7b. The number of clusters is predefined as 4, and the segmentation results of the nine algorithms are presented in Figs. 5c–k, 6c–k and 7c–k, respectively.

As is shown in Figs. 5, 6 and 7, much noise exists in the results of FCM, BCFCM, FCMS1, FCMS2, FGFCM, EnFCM, a small portion of noise exists in the results of KWFLICM, and almost all noise is removed by FLICM and NLFCM. Also, due to not considering the gray information in the fuzzy factor, many details disappear in the result of FLICM while appear in the result of NLFCM, shown in Fig. 7i and k.

To compare the algorithms quantitatively, V_{pc} and V_{pe} are adopted to measure the nine algorithms, and corresponding values on the three medical images are tabulated in Table 4. It is to be noted that the V_{pc} and V_{pe} values are the average values of 10 runs. As is shown from Table 4, NLFCM has the best V_{pc} and V_{pe} , meaning that the membership values in the proposed algorithm are more crisp.

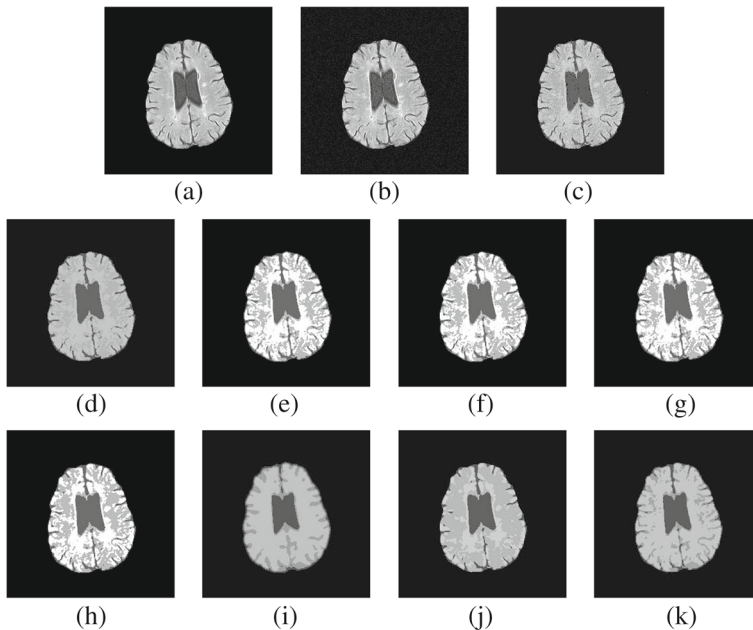


Fig. 7 Segmentation results of another medical image corrupted by 30% Rician noise. **a** Original image. **b** Noisy image corrupted by Salt & Pepper Rician noise of level 10%. **c** FCM result. **d** BCFCM result. **e** FCMS1 result. **f** FCMS2 result. **g** EnFCM result. **h** FGFCM result. **i** FLICM result. **j** KWFLICM result. **k** NLFCM result

In addition, the task of image segmentation for brain images is to partition the image into four parts: background, cerebral spinal fluid(CSF), gray matter(GRY) and white matter(WHT). Compared with the referenced images of BrainWeb, the SAs on CSF, GRY and WHT of the nine algorithms are presented in Table 5. As is shown from Table 5, the segmentation accuracy of NLFCM is higher than that of the other algorithms, meaning that the proposed algorithm is effective, and can segment corresponding tissues accurately.

4.3 Results on natural images

In this subsection, the experiments on three natural images will be illustrated. Figs. 8a and 9a with 190×123 and 189×123 pixels are from [17], while Fig. 10a with 481×321 pixels is selected from [2]. The number of clusters of the three images is assigned as 2, 3 and 2, respectively. To compare the results with other algorithms, Figs. 8a and 9a are corrupted by Salt & Pepper noise(15 %) and Gaussian noise(15 %), shown in Figs. 8b and 9b, and the salient region is required to be retrieved in Fig. 10a. The segmentation results of the nine algorithms on the three natural images are presented in Figs. 8c–k, 9c–k and 10c–k.

As is shown from Fig. 8c–h, there is still much noise in the results of FCM, BCFCM, FCMS1, FCMS2, EnFCM and FGFCM, meaning that the results of these algorithms cannot be accepted. From Fig. 8i–j we can see that two little regions exist in the segmentation results of FLICM and KWFLICM. From the segmentation results in Fig. 8 we can see that the visual effect of NLFCM is best, followed by FLICM and KWFLICM, and then the other algorithms. From Fig. 9c–k, we can see that the visual effect of FLICM, KWFLICM and NLFCM are better than the other algorithms.

Table 4 Comparison of V_{pc} and V_{pe} on medical images with Rician noise(30%)

Parameter	Image	FCM	BCFCM	FCMSI	FCMS2	EnFCM	FGFCM	FLICM	KWFLICM	NLFCM
V_{pc}	Fig. 5b	0.7775	0.4538	0.6606	0.6600	0.8054	0.8054	0.7698	0.7143	0.9111
	Fig. 6b	0.7741	0.4513	0.6450	0.6481	0.8469	0.8558	0.6263	0.7301	0.8686
	Fig. 7b	0.9195	0.8581	0.9105	0.9142	0.9344	0.9366	0.9271	0.9170	0.9488
V_{pe}	Fig. 5b	0.6050	1.3171	0.8673	0.8697	0.5190	0.5171	0.6468	0.8208	0.2532
	Fig. 6b	0.6138	1.3246	0.8952	0.8916	0.4391	0.4174	0.9193	0.7819	0.3906
	Fig. 7b	0.2363	0.3848	0.2466	0.2382	0.1789	0.1723	0.2036	0.2366	0.1510

Table 5 Comparison of SAs for Brain images with Rician noise(30%)

Image	Region	FCM	BCFCM	FCMS1	FCMS2	EnFCM	FGFCM	FLICM	KWFLICM	NLFCM
Fig. 5b	CSF	0.7533	0.7810	0.8139	0.8057	0.8451	0.8562	0.9430	0.9452	0.9459
	GRY	0.8167	0.5685	0.9137	0.9114	0.9113	0.9153	0.9286	0.9234	0.9288
	WHT	0.8620	0.9368	0.9470	0.9419	0.9486	0.9501	0.9462	0.9557	0.9488
Fig. 6b	CSF	0.7248	0.7471	0.7552	0.7516	0.9422	0.9402	0.9490	0.9495	0.9497
	GRY	0.8213	0.9205	0.9172	0.9144	0.8836	0.8768	0.9230	0.9123	0.9238
	WHT	0.8682	0.9413	0.9483	0.9461	0.9351	0.9376	0.9498	0.9540	0.9597

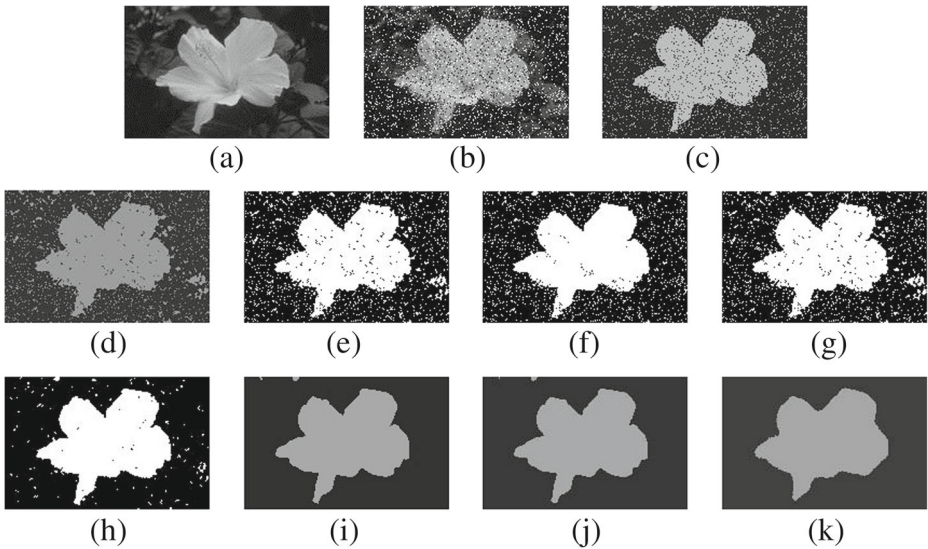


Fig. 8 Segmentation results of the first natural image. **a** Original image. **b** Noisy image corrupted by Salt & Pepper noise of level 15%. **c** FCM result. **d** BCFCM result. **e** FCMS1 result. **f** FCMS2 result. **g** EnFCM result. **h** FGFCM result. **i** FLICM result. **j** KWFLICM result. **k** NLFCM result

As can be seen from the results of Fig. 10, there are many textures in Fig. 10a, and traditional algorithms without considering texture features cannot obtain satisfying salient regions, such as FCM, BCFCM, FCMS1, FCMS2, FGFCM, shown in Fig. 10c–h. Also,

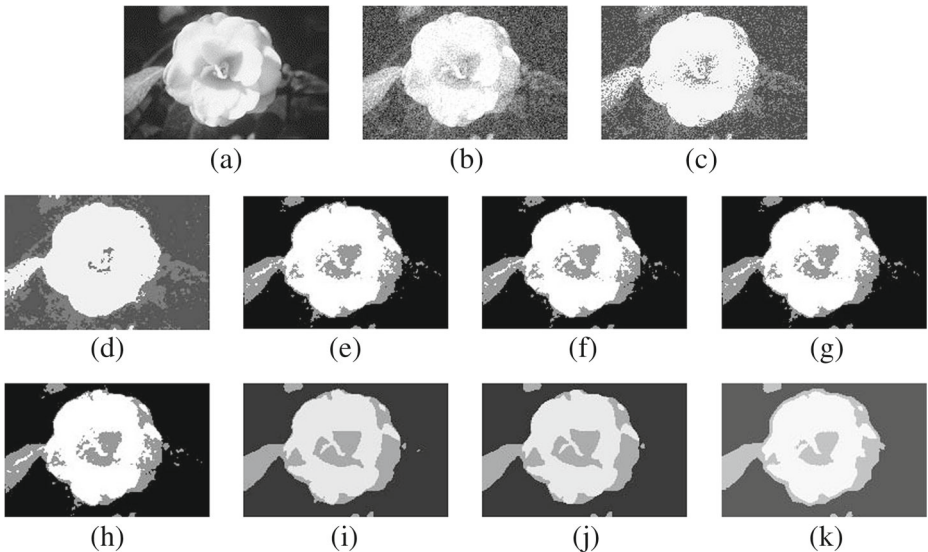


Fig. 9 Segmentation results of the second natural image. **a** Original image. **b** Noisy image corrupted by Gaussian noise of level 15%. **c** FCM result. **d** BCFCM result. **e** FCMS1 result. **f** FCMS2 result. **g** EnFCM result. **h** FGFCM result. **i** FLICM result. **j** KWFLICM result. **k** NLFCM result

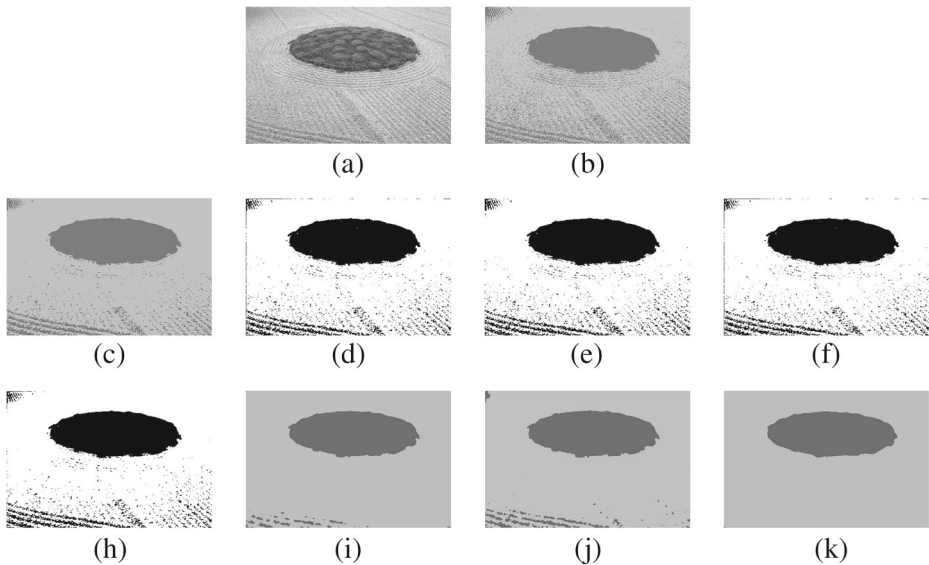


Fig. 10 Segmentation results of the third natural image. **a** Original image. **b** FCM result. **c** BCFCM result. **d** FCMS1 result. **e** FCMS2 result. **f** EnFCM result. **g** FGFCM result. **h** FLICM result. **i** KWFLICM result. **j** NLFCM result

some small regions still exist in the results of FLICM and KWFLICM, shown in Fig. 10i–j, while the salient region obtained by NLFCM is satisfying. In addition, V_{pc} and V_{pe} are compared in our experiments, and the results are presented in Table 6. As is shown in Table 6, more crisp membership values are obtained by NLFCM, resulting in higher V_{pc} and smaller V_{pe} .

4.4 Discussion of the radius of the search window

As is analyzed from NLFCM, the time complexity of the proposed algorithm is $O(n(2r + 1)^2CI)$, where I is the number of iterations. Also, with the increment of the parameter r , more non-local information will be involved in enhancing the robustness of the algorithm. However, considering more information means low efficiency. Therefore, it is not reasonable to assign the radius r too large value for the complexity of computing. In our experiments, the selection of the radius is performed by trial-and-error method, and the noise level is also considered. That is to say, when the noise level is high, one big radius is needed, and vice versa. As is shown in Fig. 3, Salt & Pepper noise is comparably more difficult to be removed than Gaussian noise. Hence, one large radius is needed when the image is corrupted by Salt & Pepper noise, resulting in low efficiency but good performance. The following figure illustrates the relationship between the radius and the segmentation result.

As is shown in Fig. 11, image artifacts exist in the segmentation result of NLFCM if the radius of the search window is assigned 1, just as the result of FLICM in Fig. 11b and b. When r is assigned 2, there are still two little noisy regions, labelled by the red box in Fig. 11d. When the radius of the search window is assigned 3, no artifacts exist in the

Table 6 Comparison of V_{pc} and V_{pe} on natural images

Parameter	Image	FCM	BCFCM	FCMS1	FCMS2	EnFCM	FGFCM	FLICM	KWFLICM	NLFCM
V_{pc}	Fig. 8b	0.9244	0.7444	0.8675	0.9089	0.9050	0.9395	0.9023	0.9473	0.9498
	Fig. 9b	0.8201	0.6810	0.8582	0.8617	0.8905	0.8955	0.9123	0.8845	0.9140
	Fig. 10a	0.8513	0.7942	0.8607	0.8590	0.8867	0.8883	0.9596	0.9189	0.9717
V_{pe}	Fig. 8b	0.2026	0.5737	0.3262	0.2250	0.2426	0.1623	0.2495	0.1438	0.1228
	Fig. 9b	0.4678	0.7773	0.3965	0.3879	0.3046	0.2917	0.2422	0.3364	0.2409
	Fig. 10a	0.3596	0.4950	0.3490	0.3531	0.2855	0.2826	0.1175	0.2236	0.0865

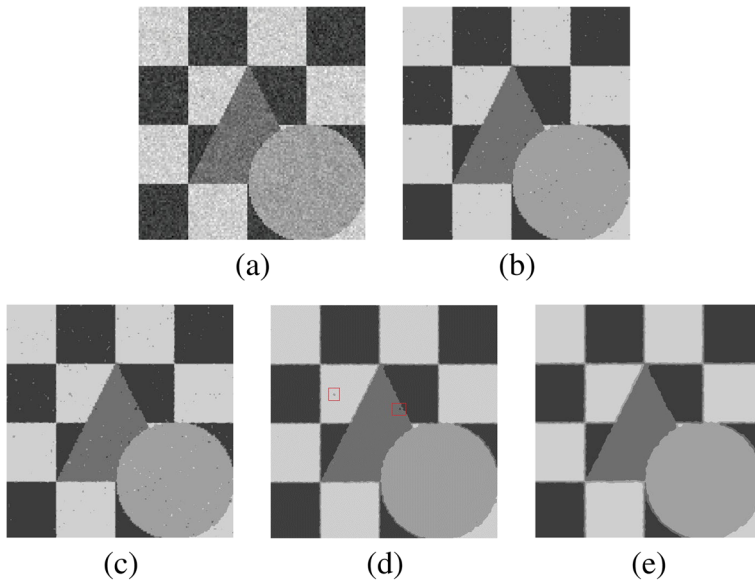


Fig. 11 Segmentation results with different radius of the search window. **a** Image corrupted by noise. **b** FLICM result. **c** NLFCM result($r = 1$). **d** NLFCM result($r = 2$). **e** NLFCM result($r = 3$)

segmentation results. In the experiments, we try to construct the relationship between the radius r and the noise degree. However, it is one difficult task. Many factors will affect the selection of the radius, such as the type of the given image, the noise degree, the type of image noise, etc. In the future work, the relationship between the radius and the noise degree will be investigated under condition that the types of image and noise are fixed, and the balance between the performance and computation cost will be also considered. Generally speaking, with the increment of the radius r , NLFCM is computationally consuming, since more pixels are involved in computing the pixel relevance and the fuzzy factor has to be computed in each iteration. However, this drawback can be compensated for its good performance, as is illustrated above.

5 Conclusion

In this paper, one improved fuzzy clustering algorithm named NLFCM is proposed, which is on the basis of FLICM and free of parameters. In the proposed algorithm, pixel relevance is computed based on the similarity of image patches, and with the help of pixel relevance, non-local information can be adopted to guide the procedure of image segmentation. As a result, the robustness of the algorithm can be enhanced greatly. Experimental results on synthetic, medical and natural images show that the proposed algorithm can improve the performance of image segmentation, and can remove noise of any type.

Acknowledgment The authors would like to thank anonymous referees for their valuable comments and suggestions which lead to substantial improvements of this paper. Also, the authors would like to thank Dr. Krindis and Dr. Maoguo GONG for providing the source codes and experimental pictures of

FLICM and KWFLICM. We would also thank Dr. Weiling CAI for providing the codes of FCMS1, FCMS2 and GFPCM. The research was supported by NSF of China (61232016, U1405254, 61373078, 61472220, 61502218), the Priority Academic Program Development of Jiangsu Higher Education Institutions, Jiangsu Collaborative Innovation Center on Atmospheric Environment and Equipment Technology, NSF of Shandong Province (ZR2014FM005), Key Technology Research and Development Program of Shandong Province (2015GSF116001, 2015GGX101004), Shandong Province Higher Educational Science and Technology Program (J14LN20), and Doctoral Foundation of Ludong University (LY2015035).

References

- Ahmed MN, Yamany SM, Mohamed N, Farag AA (2002) A modified fuzzy C-mean algorithm for bias field estimation and segmentation of MRI data. *IEEE Trans Med Imaging* 21(3):193–199
- Besser H (1990) Visual access to visual images: the UC Berkeley Image Database Project. *Library Trends* 38(4):787–798
- Bezdek J (1975) Mathematical models for systematics and taxonomy[C] 3:143–166. Proceedings of eighth international conference on numerical taxonomy
- Bezdek J (1975) Cluster validity with fuzzy sets. *J Cybern* 3(3):58–73
- Bezdek J (1980) A convergence theorem for the fuzzy ISODATA clustering algorithms. *IEEE Trans Pattern Anal Mach Intell* 2(1):1–8
- Bezdek J (1981) Pattern recognition with fuzzy objective function algorithms. Plenum, New York
- Bezdek J, Hall L, Clarke L (1992) Review of MR image segmentation techniques using pattern recognition. *Medical physics* 20(4):1033–1048
- Cai W, Chen S, Zhang D (2007) Fast and robust fuzzy C-means clustering algorithms incorporating local information for image segmentation. *Pattern Recogn* 40:825–838
- Chen S, Zhang D (2004) Robust image segmentation using fcm with spatial constraints based on new kernel-induced distance measure. *IEEE Trans Syst Man Cybern Part B Cybern* 34:1907–1916
- Cocosco C, Kollokian V, Kwan R et al BrainWeb: Online interface to a 3D MRI simulated brain database[Online]. Available: <http://www.bic.mni.mcgill.ca/brainweb/>
- Dunn J (1974) A fuzzy relative of the ISODATA process and its use in detecting compact well separated clusters. *J. Cybern* 3:32–57
- Gong M, Liang Y, Shi J, Ma W, Ma J (2013) Fuzzy C-means clustering with local information and kernel metric for image segmentation. *IEEE Trans Image Process* 22(2):573–584
- Gong M, Zhou Z, Ma J (2012) Change detection in synthetic aperture radar images based on image fusion and fuzzy clustering. *IEEE Trans Image Process* 21(4):2141–2151
- Ji Z, Sun Q, Xia D (2010) A modified possibilistic fuzzy C-means clustering algorithm for bias field estimation and segmentation of brain MR image. *Comput Med Imaging Graph* 35:383–397
- Ji Z, Sun Q, Xia D (2011) A framework with modified fast FCM for brain MR images segmentation. *Pattern Recogn* 44:999–1013
- Jian M, Lam K, Dong J, Shen L (2015) Visual-patch-attention-aware Saliency Detection. *IEEE Transactions on Cybernetics* 45(8):1575–1586
- Krinidis S, Chatzis V (2010) A Robust Fuzzy Local Information C-means Clustering Algorithm. *IEEE Trans Image Process* 19(5):1328–1337
- Li J, Li X, Yang B, Sun X (2015) Segmentation-based Image Copy-move Forgery Detection Scheme. *IEEE Trans Inf Forensics Secur* 10(3):507–518
- MathWorks Image Processing Toolbox, Natick, MA[Online]. Available: <http://www.mathworks.com/matlabcentral/fileexchange/14237>
- Pham D (2001) Robust fuzzy segmentation of magnetic resonance images. In: Proceedings of the 14th IEEE Symposium on Computer-Based Medical Systems, pp 127–131
- Pham D (2001) Spatial models for fuzzy clustering. *Comput Vis Image Underst* 84(2):285–297
- Pham D, Prince J (1999) An adaptive fuzzy C-means algorithm for image segmentation in the presence of intensity inhomogeneities. *Pattern Recogn Lett* 20(1):57–68
- Roy S, Agarwal H, Carass A, Bai Y, Pham D (2008) J Prince. Fuzzy C-means with variable compactness. 5th IEEE International Symposium on Biomedical Imaging: From Nano to Macro:452–455
- Sun Y, Dong J, Jian M et al (2015) Fast 3D face reconstruction based on uncalibrated photometric stereo. *Multimedia Tools and Applications* 74(11):3635–3650
- Szilágyi L, Benyó Z, Szilágyi SM, Adam HS (2003) MR Brain image segmentation using an enhanced fuzzy C-means algorithm. In: Proceeding of 25th Annual International Conference of IEEE EMBS, pp 17–21

26. Wang G, Zhang X, Su Q et al (2015) A novel cortical thickness estimation method based on volumetric Laplace-Beltrami operator and heat kernel. *Med Image Anal* 22:1–20
27. Zhang X, Wang G, Su Q et al An improved fuzzy algorithm for image segmentation using peak detection, spatial information and reallocation. *Soft Comput*. doi:[10.1007/s00500-015-1920-1](https://doi.org/10.1007/s00500-015-1920-1)
28. Zhao F (2013) Fuzzy clustering algorithms with self-tuning non-local spatial information for image segmentation. *Neurocomputing* 106:115–125
29. Zhao F, Jiao L, Liu H (2011) Fuzzy C-means clustering with non local spatial information for noisy image segmentation. *Frontiers of Computer Science in China* 5(1):45–56
30. Zheng Y, Jeon B, Xu D, Jonathan W, Zhang H (2015) Image segmentation by generalized hierarchical fuzzy C-means algorithm. *J Intell Fuzzy Syst* 28(2):961–973



Xiaofeng Zhang received the B.S. degree and the Master Degree from School of Computer and Communication, Lanzhou University of Technology, Lanzhou, China, in 2000 and 2005, respectively. He received the Ph.D. Degree from School of Computer Science and technology, Shandong University, Jinan, China, in 2014. Now he is an associate professor with the School of Information and Electrical Engineering, Ludong University, and with Shandong Provincial Key Laboratory of Digital Media Technology. His research interest includes image segmentation, sparse representation, etc.



Yujuan Sun is a lecturer in the College of Information and Electrical Engineering at Ludong University of China. She was awarded a Ph.D. degree in Image Processing in 2014 from the Department of Computer Science and Technology, Ocean University of China. Yujuan Sun has published more than 20 journal and international conference papers (indexed by SCI and EI). Her research interests include 3D shape reconstruction from images, pattern recognition, and machine learning.



Gang Wang received the Master Degree of Engineering from University of Electronic Science and Technology of China in 2004, and received the Ph.D. degree from Nanjing University of Science and Technology in 2007. He is working as a professor in School of Information and Electric Engineering of Ludong University, Yantai, China. His research interests include multiscale geometry analysis, image sparse decomposition, partial differential equation, fractal and image statistical modeling.



Qiang Guo received the B.S. degree in information and computing science from Shandong University of Technology, Zibo, China, in 2002, the M.S. and Ph.D. degrees in computer science from Shanghai University, Shanghai, China, in 2005 and 2010, respectively. From 2013 to 2015, he was a Post-Doctoral Fellow with the School of Computer Science and Technology, Shandong University, China. He is currently an Associate Professor with the School of Computer Science and Technology, Shandong University of Finance and Economics, and with Shandong Provincial Key Laboratory of Digital Media Technology. His current research interests include image restoration, sparse representation, and object detection.



Caiming Zhang is a professor and doctoral supervisor of the school of computer science and technology at the Shandong University. He is now also the dean and professor of the school of computer science and technology at the Shandong University of Finance and Economics. He received a BS and an ME in computer science from the Shandong University in 1982 and 1984, respectively, and a Dr. Eng. degree in computer science from the Tokyo Institute of Technology, Japan, in 1994. From 1997 to 2000, Dr. Zhang has held visiting position at the University of Kentucky, USA. His research interests include CAGD, CG, information visualization and medical image processing.



Beijing Chen received the Ph.D.degree in Computer Science in 2011 from South east University, Nanjing, China. Now he is an associate professor in the School of Computer & Software, Nanjing University of Information Science & Technology, China. His research interests include color image processing, information security and pattern recognition.